The Successful Operation of Hole-Type Gaseous Detectors at Cryogenic Temperatures

L. Periale, V. Peskov, C. Iacobaeus, T. Francke, B. Lund-Jensen, P. Pavlopoulos, P. Picchi, F. Pietropaolo, and F. Tokanai

***Abstract*—We have demonstrated that hole-type gaseous detectors, gas electron multipliers and capillary plates (CPs) can operate at temperatures down to 77 K. For example, a single CP can operate at gains above 10^3 in the entire temperature interval between 77 and 300 K. The same CP combined with CsI photocathodes operates perfectly well at gains of 100–1000, depending on the gas mixture. The obtained results open new fields of applications for CPs as detectors of ultraviolet light and charged particles at cryogenic temperatures: liquid noble gas time-projection chambers, detectors for weakly interacting massive particles or liquid Xe scintillating calorimeters, and cryogenic positron-emission tomography.**

***Index Terms*—CsI photocathode, noble liquids, TCP.**

I. Introduction

IN SEVERAL studies and applications, there is a great need for the detection of vacuum ultraviolet (VUV) light at cryogenic temperatures. Examples are high-energy physics and astrophysics experiments [1], liquid noble gas positron-emission tomography [2], studies of cryogenic plasmas, and studies of quantum phenomena in liquid and solid He [3]. Focusing on high-energy physics, one of the main applications could be the liquid noble gas time-projection chambers (TPCs) and liquid noble gas scintillation calorimeters [4]. TPCs are rather widely used detectors: the ICARUS experiment [1], the nTOF experiment [5], and liquid Xe/Ar detectors for weakly interacting massive particles search [6] are all good examples.

A cryogenic TPC is usually a large-volume structure filled with liquid noble gas (see Fig. 1). If an interaction occurs inside the liquid, scintillation light and an ionization track from a charged particle are produced simultaneously. The scintillation light is detected by photodetectors. By influence of the external electric field, parts of the primary electrons from the track are collected on the position-sensitive readout plate. This allows obtaining a two-dimensional (2-D) projection of the track. The time difference between the scintillation light and the charge collection on the position-sensitive elements is used for the 3-D track reconstruction. A liquid noble gas TPC is a very powerful detector, not only to visualize the tracks, but also to measure the deposited energy and perform event rejection from the measured light-to-charge ratio, a usage for which photodetectors are important components of the TPCs. Until now, vacuum photomultipliers (PMs) have usually been used.

In a recent publication [7], some preliminary results were presented demonstrating that gaseous detectors with highly efficient solid photocathodes can operate at low temperatures. This opens the possibility of replacing costly and bulky PMs with cheap and simple photosensitive gaseous detectors. One can also note that gaseous detectors are less sensitive to magnetic fields, as desired for some experiments.

In this paper, we present new results from systematic studies of the operation of gaseous detectors at cryogenic temperatures obtained with the latest equipment.

II. Experimental Setup

The experimental setup is shown schematically in Fig. 2. It consists of a cryostat with a test chamber located inside (see also Fig. 3). The cryostat was originally designed for tests of the ATLAS barrel presampler. It uses a computer-controlled temperature regulator to open or close a valve on the liquid nitrogen inlet tube. This allows cooling to any temperature between 290 K and liquid nitrogen (LN_2)'s temperature with a selected time profile. The test chamber was filled with Ar $+10\%CH_4$ or He $+10\%H_2$ gas mixtures at a pressure of 1 atm. We chose these mixtures because they contained quenchers which remained in gas phase at low temperatures: $T > 170$ K for Ar + CH_4, and $T > 78$ K for He + H_2. Some tests were also done with pure noble gases. If necessary, a gas scintillation chamber, filled with Ar or Kr at 1 atm, could be attached to the test chamber via a MgF_2 window (see Fig. 2). The scintillation light was produced by an alpha source placed inside. Inside the test chamber, various gaseous detectors could be installed. The main focus in these studies was on the hole-type detectors because of their unique properties, which are the ability to operate in poorly quenched gas mixtures and the possibility of working in cascade mode. The hole-type detectors used in these studies were gas electron multipliers (GEMs) or capillary plate (CP). GEMs had sizes of 5×5 cm^2 and hole pitches (50 μm in diameter) of 140 μm. GEMs were used either in CAT (the

Manuscript received November 14, 2004; revised March 14, 2005.

L. Periale and P. Pichi are with CERN, Geneva CH-1211, Switzerland. They are also with IFSI-CNR Torino, Torino I-10133, Italy (e-mail: Luciano.Periale@cern.ch; Pio.Picchi@cern.ch).

V. Peskov is with the Research Division, Léonard de Vinci University, 92916 Paris La Defanse, France (e-mail: Vladimir.peskov@cern.ch).

C. Iacobaeus is with the Medical Radiation Physics Department, Karolinska Institutet, S-17176 Stockholm, Sweden (e-mail: Christian@radfys.ki.se).

T. Francke is with XCounter AB, S-18233 Danderyd, Sweden (e-mail: tom.francke@xcounter.se).

B. Lund-Jensen is with the Physics Department, Royal Institute of Technology, S-10692 Stockholm, Sweden (e-mail: lund@particle.kth.se).

P. Pavlopoulos is with the Research Division, Léonard de Vinci University, 92916 Paris La Defanse, France. He is also with CERN, Geneva CH-1211, Switzerland (e-mail: Noulis.Pavlopoulos@devinci.fr).

F. Pietropaolo is with CERN, Geneva CH-1211, Switzerland. He is also with INFN, Padova I-35131, Italy (e-mail: Francesco.Pietropaolo@cern.ch).

F. Tokanai is with Yamagata University, Yamagata 990-8560, Japan (e-mail: tokanai@sci.kj.yamagata-u.ac.jp).

Digital Object Identifier 10.1109/TNS.2005.852632

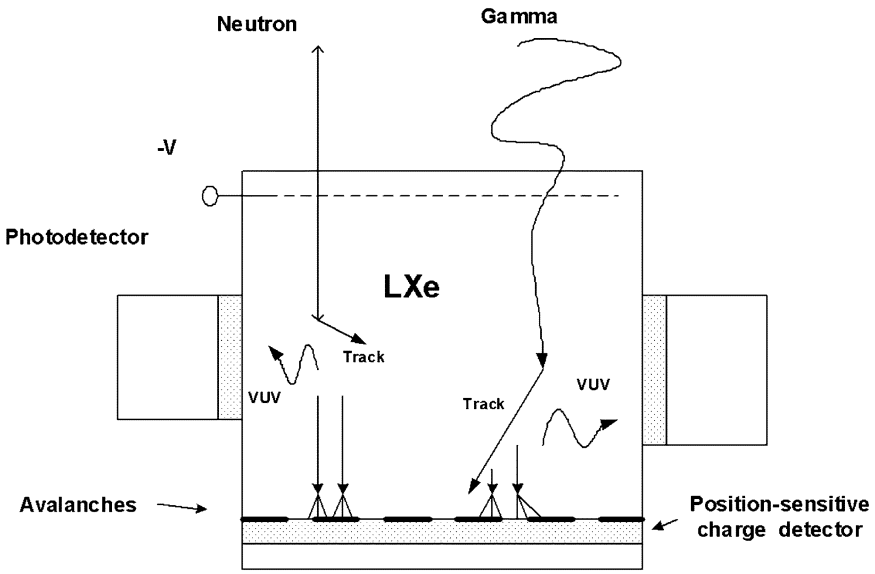

Fig. 1. Schematic drawing illustrating the operational principle of a noble liquid TPC.

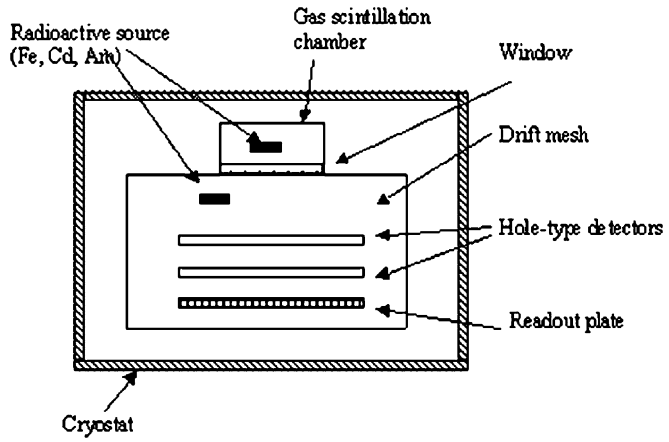

Fig. 2. Schematic drawing of the experimental setup for measurements with radioactive sources.

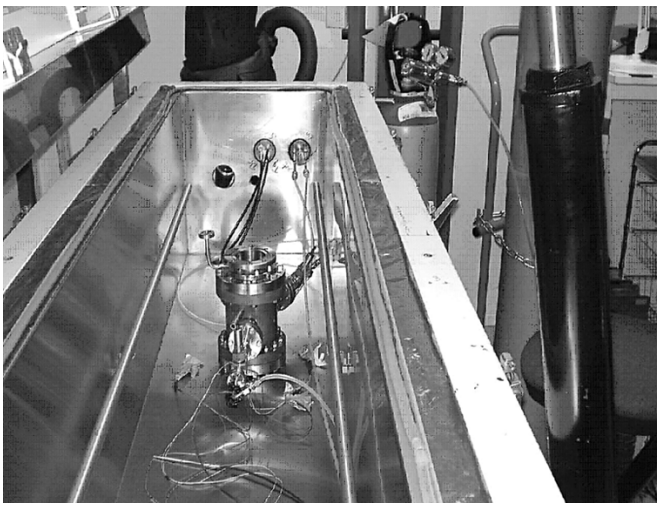

Fig. 3. Photo of the cryostat with the test chamber inside.

cathode was electrically connected to the readout plate placed in contact) or cascade mode (two GEMs). The diameter of the CPs

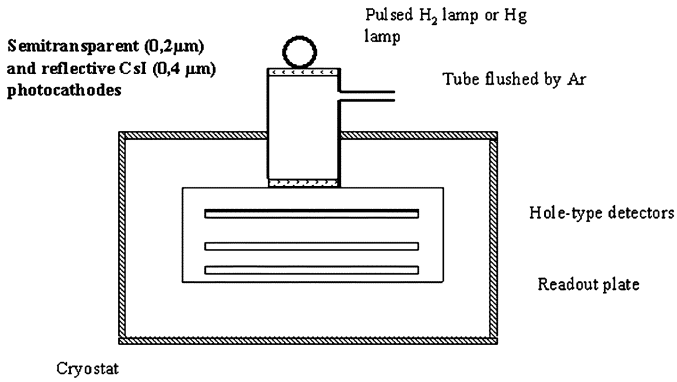

Fig. 4. Setup modifications for measurements with external UV sources.

used was 20 mm. Two thicknesses were tested: 0.4 and 0.8 mm. The capillary holes had a diameter of 40 or 100 μm and an open area ratio of 57%.

The operation of these detectors in combination with CsI and other solid photocathodes was also studied (see [8] for more details). For these measurements, the test chamber was slightly modified, as shown in Fig. 4. In this paper, we only present selected results obtained with reflective and semitransparent CsI photocathodes. Semitransparent CsI (20-nm thickness) was deposited on the inner surface of the MgF_2 window. In the case of the reflective photocathode, CsI was deposited on the top electrode of the hole-type detector (the thickness was 400 nm).

It is known that gaseous detectors combined with CsI photocathodes, even at low gains (A), may suffer from feedback problems: an appearance of undesirable successive pulses followed the real signal (see [9] and [10]). For feedback measurements, a pulsed (a few ns) H_2 lamp was placed outside the cryostat (see Fig. 4). The same lamp in combination with an Hg lamp was also used for the quantum efficiency measurements [7].

The signals from the capillaries were read out by a charge-sensitive amplifier (Ortec, 142 PC). In some measurements, we also recorded pulse-height spectra produced by radioactive sources or by an H_2 lamp (see [8] for more details).

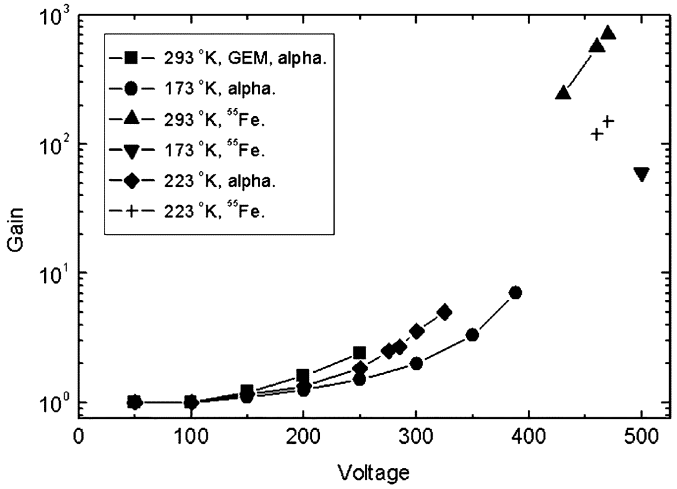

Fig. 5. GEM gains (CAT mode) measured with alphas ($A < 10$) and with ^{55}Fe ($A > 40$) in Ar $+10\%$CH$_4$ at various temperatures.

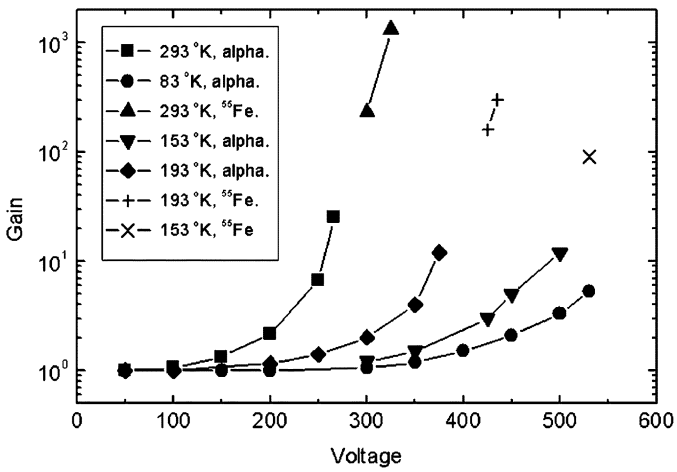

Fig. 6. GEM gains (CAT mode) measured with alphas ($A < 20$) and ^{55}Fe ($A > 100$) in He $+10\%$H$_2$ at various temperatures.

III. Results

A. Gain Measurements With Radioactive Sources

Figs. 5 and 6 show the gain measurements of a single GEM operating in Ar + CH$_4$ and He + H$_2$ gas mixtures at $P = 1$ atm. At low gas gains ($A < 10$), measurements were done with the alpha source (^{241}Am) and at high gains with ^{55}Fe. The measurements with the ^{55}Fe were stopped at the voltage where some instability or predischarges appeared. One can see that the maximum achievable gain of the GEM dropped sharply with the temperature; however, it could still operate, even at an LN$_2$ temperature.

Figs. 7 and 8 show the gain of the CPs in He + H$_2$ and Ar + CH$_4$ mixtures at various temperatures. One can see that the maximum achievable gain of the CPs is much higher than for the GEMs, although it drops with the temperature, as well. Note that CPs could operate at gains of 10^3, even in pure Ar (see [7] for more details). In discharge-rate studies, the gain was kept a factor 5 below the breakdown limit. In this case, discharge rates were less than one in the period of 1–2 hours. Since the counting rate in our measurements was 1000 Hz, the discharge rate was below 3×10^{-8}.

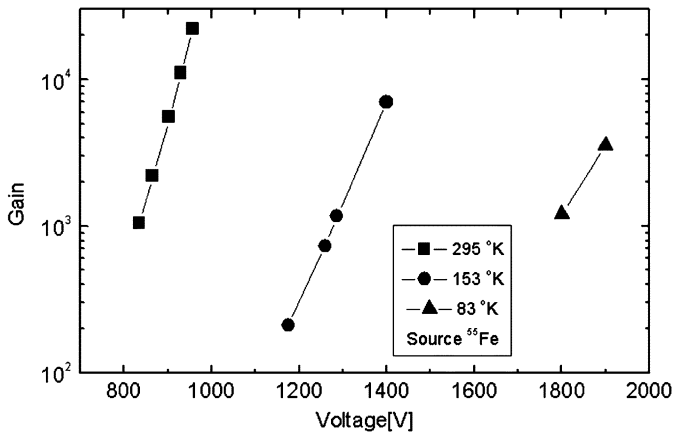

Fig. 7. CP gains measured with ^{55}Fe in He $+10\%$H$_2$ at 183 and 295 K.

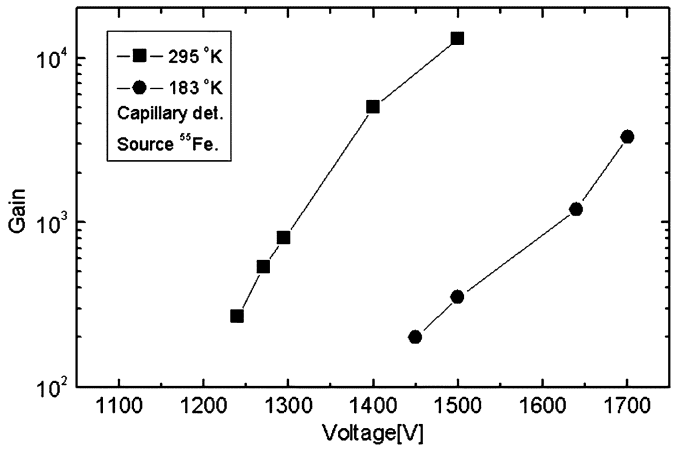

Fig. 8. Gains (^{55}Fe) of conventional CPs in Ar + CH$_4$ at several temperatures.

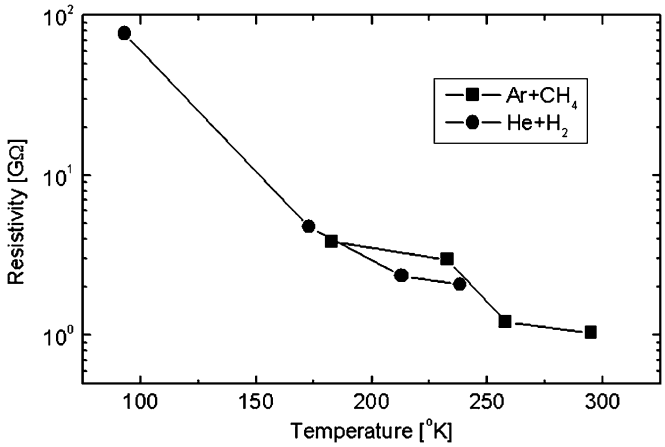

Fig. 9. Resistivity of an H$_2$-treated CP versus the temperature in Ar $+10\%$CH$_4$ and He $+10\%$H$_2$ gas mixtures.

The operation of H$_2$-treated CPs were also tested. An advantage of this type of CP is its ability to operate at high counting rates [11]. Fig. 9 shows how their resistivity changes with the temperature. The resistivity measured between the electrodes of the H$_2$-treated CP was ~ 1 GΩ at 293 K. At this temperature, the resistivity obeyed Ohm's Law. At LN$_2$ temperature,

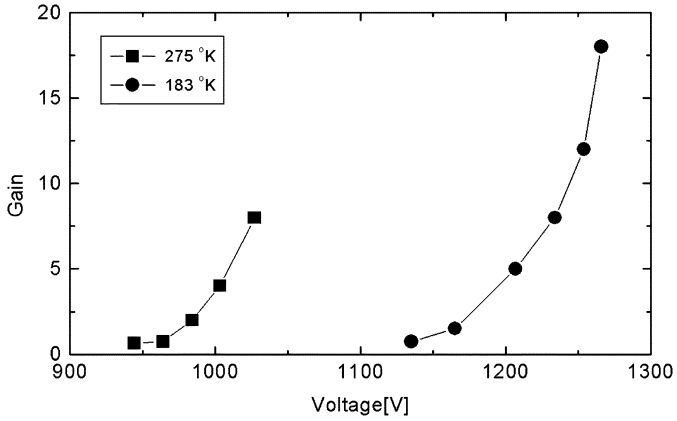

Fig. 10. Alpha signals measured on the readout plate of the hydrogen-treated CP (in the charge-extraction mode) in Ar + CH_4 at 183 and 275 K.

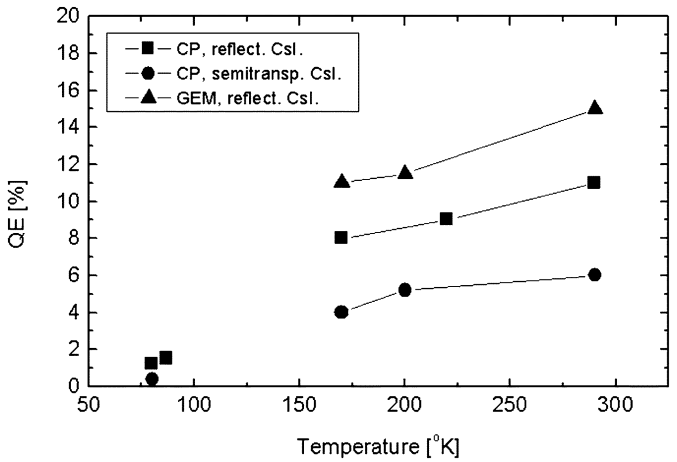

Fig. 11. QE of hole-type detectors measured at various temperatures in Ar $+10\%CH_4$ ($T > 150$ K) and He $+10\%H_2$ ($T < 100$ K) gas mixtures. Triangles: GEM with reflective CsI photocathode. Squares: CPs with reflective CsI photocathode. Circles: CPs with semitransparent CsI photocathodes.

the resistivity reached ~ 100 GΩ, and began to deviate from Ohm's Law. This value of resisitivity is still, by a few orders of magnitude, less than the conventional (untreated by H_2) CPs. Thus, rate characteristics of cooled H_2-treated CPs are superior. Gain curves for the H_2-treated CPs measured with alpha sources in the charge-extracted mode are presented in Fig. 10. In these tests, we used only alpha sources, thus, the maximum achievable gain was several orders of magnitude lower than in the case of the ^{55}Fe source (see Section IV).

B. Quantum Efficiency and Gain Measurements With Hole-Type Gaseous Detectors Combined With Reflective and Semitransparent Photocathodes

The procedure of the CsI quantum efficiency (QE) calibration is described in [7]. In these measurements, the gain of the CPs and GEMs were kept much lower than the breakdown limit, so the results from the QE measurements presented here correspond to the low-gain case.

The QE of hole-type detectors in Ar $+10\%CH_4$ and He $+10\%H_2$ gas mixtures, and at various temperatures, are presented in Fig. 11. One can see that the value of the QE was,

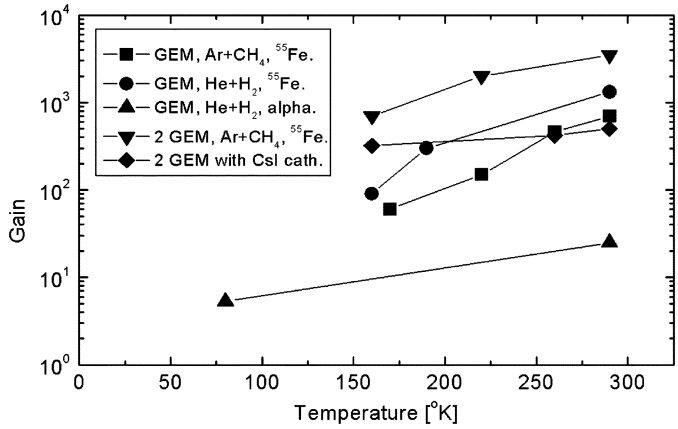

Fig. 12. Summary of results obtained with GEMs. Single and double GEM gains with and without CsI photocathodes. Squares: single GEM in Ar + CH_4 (^{55}Fe). Circles: single GEM in He + H_2 (^{55}Fe). Upward triangles: single GEM in He + H_2 (alpha). Downward triangles: double GEMs in Ar $+10\%CH_4$ (^{55}Fe). Rhombus: double GEM with a reflective CsI photocathode.

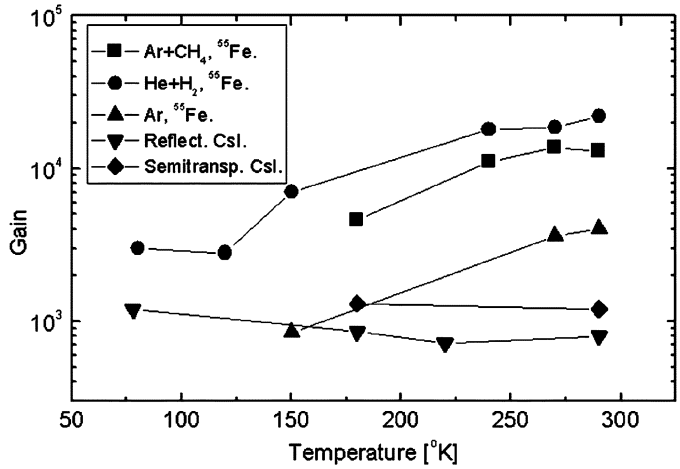

Fig. 13. Summary of results obtained with CPs. Single CP gains with and without CsI photocathodes. Squares: bare CP in Ar + CH_4 (^{55}Fe). Circles: bare CP in He + H_2 (^{55}Fe). Upward triangles: bare CP in Ar (^{55}Fe). Downward triangles: CP with a reflective CsI photocathode. Rhombus: CP with a semitransparent CsI photocathode.

depending on the detector, between 14% and 5%. Note: the heavy loss of the measured efficiency at $T \sim 80$ K is due to the strong back diffusion of the photo electrons in the He + H_2 gas mixture [7] (which is much stronger than in the Ar + CH_4 gas mixture). The absolute QE of the CsI itself remains almost unchanged with the temperature [7].

Figs. 12 and 13 summarize our results obtained with GEMs and CPs. One can see that in both cases, the maximum achievable gain of the detectors dropped with the temperature, but the maximum achievable gain with the CsI photocathode remains almost unchanged. Photosensitive gaseous detectors are thus able to operate at high gains, even at cryogenic temperatures. Note also that CPs offer higher gains, compared with GEMs.

IV. Discussion and Conclusions

We have experimentally demonstrated that both GEMs and CPs can operate at cryogenic temperatures down to 78 K. CPs offer the highest gains possible in a single-step operating mode,

and can thus be used to detect charges at cryogenic temperatures, for example, in WIMP detectors operating in a charge-extracting mode [12].

The fact that CPs offer higher gains than the GEMs, and that the maximum achievable gain $A_{\max}$ for both types of detectors dropped with decreasing temperature, can be explained by results presented in our earlier work [13]. There it was shown that the maximum achievable gain of bare hole-type detectors is

$$A_{\max} = \frac{Q(\rho, \Delta)}{n_0} \tag{1}$$

where $Q(\rho, \Delta)$ is a constant depending on the gas density ρ and the detector thickness Δ, and n_0 is the number of primary electrons created by the radioactive source (^{55}Fe, or alphas in our case). Usually, $Q(\rho, \Delta)$ drops with decreasing thickness of the amplification gap, and also with the gas density. This is why one can reach higher gains with the CPs than with the GEMs, and why the maximum achievable gains of hole-type detectors drops with the temperature.

The other important result is that GEMs and CPs combined with the CsI photocathodes can also operate at cryogenic temperatures, however, with a lower maximum achievable gain. In the case of the CPs or the GEMs combined with photocathodes, $A_{\max}$ is limited by feedback processes [14]

$$A_{\max}\gamma = 1 \tag{2}$$

where γ is the probability of the secondary electron appearance due to the feedback mechanisms [9], [10]. Usually, γ drops with the pressure [15], so that $A_{\max}$ stays almost unchanged with decreasing temperature, or even slightly increases (see Fig. 13).

The value of the QE at cryogenic temperatures is found to be high enough to use these detectors as alternatives to PMs. This opens new avenues in applications, such as in the readout of liquid noble gas TPCs.

Note that photosensitive gaseous detectors has already successfully been used in the detection of the scintillation lights from gaseous or liquid noble gases [7].

REFERENCES

[1] C. Montanari, "The ICARUS project. A 3000 ton detector for neutrino and matter stability searches," *Nucl. Instrum. Phys. Res.*, vol. A518, pp. 216–219, Feb. 2004.

[2] V. Chepel, M. Lopes, A. Kuchenkov, R. F. Marques, and A. Policarpo, "Performance study of LXe detector for PET," *Nucl. Instrum. Phys. Res.*, vol. A392, pp. 427–432, Jun. 1997.

[3] W. F. Schmidt, *Liquid State Electronics of Insulating Liquids*. Boca Raton, FL: CRC Press, 1997.

[4] D. Akimov *et al.*, "Development of LXe/LKr electromagnetic calomiter with wavelength shifting light collection," *Nucl. Instrum. Phys. Res.*, vol. A379, pp. 484–487, Sep. 1996.

[5] P. Pavlopoulos, "The nTOF status report,", Rep. CERN/INTC 2001-021, 2001.

[6] E. Aprile, "XENON: A liquid xenon experiment for dark matter," Columbia Univ., New York, NY, NSF Proposal 0201740.

[7] L. Periale, V. Peskov, C. Iacobaeus, T. Francke, B. Lund-Jensen, N. Pavlopoulos, P. Picchi, and F. Pietropaolo, "The development of gaseous detectors with solid photocathodes for low temperature applications," *Nucl. Instrum. Phys. Res.*, vol. A535, pp. 517–522, Sep. 2004.

[8] L. Periale, V. Peskov, C. Iacobaeus, T. Francke, B. Lund-Jensen, N. Pavlopoulos, P. Picchi, F. Pietropaolo, and F. Tokanai, "A systematic study of operation of photosensitive gaseous detectors at cryogenic temperatures," *Physics*, submitted for publication.

[9] P. Fonte, V. Peskov, and F. Sauli, "Feedback and breakdown in parallel-plate chambers," *Nucl. Instrum. Phys. Res.*, vol. A305, pp. 91–110, Jan. 1999.

[10] G. Charpak, P. Fonte, V. Peskov, F. Sauli, and D. Scigocki, "Investigation of operation of a parallel-plate avalanche chamber with a CsI photocathode under high gain conditions," *Nucl. Instrum. Phys. Res.*, vol. A307, pp. 63–68, Feb. 1991.

[11] J. Ostling, A. Brahme, M. Danielsson, T. Francke, C. Iacobaeus, and V. Peskov, "Study of hole-type gas multiplication structures for portal imaging and other high count rate applications," *IEEE Trans. Nucl. Sci.*, vol. 50, no. 4, pp. 809–819, Aug. 2003.

[12] A. Bondar *et al.*. Cryogenic avalanche detectors based on gas electron multiplier. [Online]. Available: http://vci.oeaw.ac

[13] V. Peskov *et al.*, "The study and optimization of new micropattern gaseous detectors for high-rate applications," *IEEE Trans. Nucl. Sci.*, vol. 48, no. 4, pp. 1070–1074, Aug. 2001.

[14] C. Iacobaeus, T. Francke, M. Danielsson, J. Ostling, and V. Peskov, "Study of capillary-based gaseous detector," *IEEE Trans. Nucl. Sci.*, vol. 51, no. 3, pp. 952–959, Jun. 2004.

[15] V. Peskov, "Secondary processes in a gas counter I," *Sov. Phys. Tech. Phys.*, vol. 20, pp. 791–794, 1975.